The HEVI approach with an IMEX-RK Discontinuous Galerkin solver

PDEs on the sphere
Montreal, Canada
29 April – 3 May 2019

Michael Baldauf
Deutscher Wetterdienst, Germany

with thanks to Floran Prill for several discussions

Discontinuous Galerkin (DG) methods in a nutshell

$$\frac{\partial q^{(k)}}{\partial t} + \nabla \cdot \mathbf{f}^{(k)}(q) = S^{(k)}(q), \qquad k = 1, ..., K$$

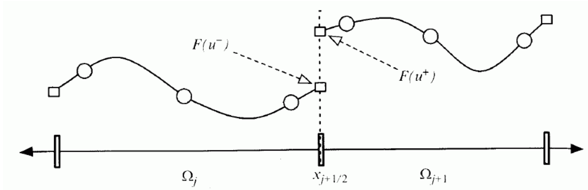

From *Nair et al. (2011)* in *‚Numerical techniques for global atm. models'*

weak formulation $\int_{\Omega_j} dx\, v(\mathbf{x}) \cdot \ldots$

Finite-element ingredient

$$q^{(k)}(x,t) = \sum_{l=0}^{p} q_{j,l}^{(k)}(t)\, p_l(x - x_j)$$

e.g. Legendre-Polynomials

e.g.
Cockburn, Shu (1989) Math. Comput.
Cockburn et al. (1989) JCP
Hesthaven, Warburton (2008): Nodal DG Methods

Finite-volume ingredient

$$\mathbf{f}(q) \rightarrow \mathbf{f}^{num}(q^+, q^-) = \frac{1}{2}\left(\mathbf{f}(q^+) + \mathbf{f}(q^-) - \alpha(q^+ - q^-)\right)$$

Lax-Friedrichs flux

Gaussian quadrature for the integrals of the weak formulation

→ ODE-system for $q^{(k)}{}_{jl}$

DG – Pros and Cons

- **local conservation**
- any **order of convergence** possible
- flexible application on **unstructured grids** (also dynamic adaptation is possible, h-/p-adaptivity)
- very good **scalability**
- **explicit** schemes are easy to build and are quite well understood
- higher accuracy helps to **avoid several awkward approaches** of standard 2nd order schemes: staggered grids (on triangles/hexagons, vertically heavily stretched), numerical hydrostatic balancing, grid imprints by pentagon points or along cubed sphere lines, …

- high computational costs due to
  - (apparently) **small Courant numbers**
  - higher number of DOFs
- **well-balancing** (hydrostatic, perhaps also geostrophic?) in Euler equations is an issue (see below)
- basically ‚only' an **A-grid-method**, however, the ‚spurious pressure mode' is very selectively damped!

Target system: **ICON model**
(Zängl et al. (2015) QJRMS)
- operational at DWD since Jan. 2015
  (global (13km) and nest over Europe (6.5km))
- convection-permitting (2.2km): Q4/2020

but currently far away from this, only a **toy model for 2D problems exists** with:

- explicit time integration DG-RK (with Runge-Kutta schemes) or horizontally explicit-vertically implicit (DG-HEVI) (with IMEX-Runge-Kutta)
- ‚local DG' (LDG) option for PDEs with higher spatial derivatives

2D Euler equations, non-hydrostatic, compressible with a reference state, in terrain-following coordinates (x, z‘)

use a *strong conservation form* with terrain following coordinates but cartesian base vectors (*Schuster et al. (2014) MetZ, appendix, for the sphere):*

$$
\begin{aligned}
\frac{\partial \tilde\rho'}{\partial t} + \frac{\partial}{\partial x}(\tilde M_x) \quad\quad + \frac{\partial}{\partial z'}\left(\frac{\partial z'}{\partial x}\tilde M_x + \frac{\partial z'}{\partial z}\tilde M_z\right) &= 0, \\
\frac{\partial \tilde M_x}{\partial t} + \frac{\partial}{\partial x}\left(\frac{\tilde M_x^2}{\tilde\rho} + \tilde p'\right) + \frac{\partial}{\partial z'}\left(\frac{\partial z'}{\partial x}\left(\frac{\tilde M_x^2}{\tilde\rho} + \tilde p'\right) + \frac{\partial z'}{\partial z}\frac{\tilde M_x \tilde M_z}{\tilde\rho}\right) &= 0, \\
\frac{\partial \tilde M_z}{\partial t} + \frac{\partial}{\partial x}\left(\frac{\tilde M_x \tilde M_z}{\tilde\rho}\right) + \frac{\partial}{\partial z'}\left(\frac{\partial z'}{\partial x}\frac{\tilde M_x \tilde M_z}{\tilde\rho} + \frac{\partial z'}{\partial z}\left(\frac{\tilde M_z^2}{\tilde\rho} + \tilde p'\right)\right) &= -g\tilde\rho' - \frac{\tilde M_z}{\tau}, \\
\frac{\partial \tilde\eta'}{\partial t} + \frac{\partial}{\partial x}\left(\frac{\tilde\eta \tilde M_x}{\tilde\rho}\right) \quad\quad + \frac{\partial}{\partial z'}\left(\frac{\partial z'}{\partial x}\frac{\tilde\eta \tilde M_x}{\tilde\rho} + \frac{\partial z'}{\partial z}\frac{\tilde\eta \tilde M_z}{\tilde\rho}\right) &= 0,
\end{aligned}
$$

$$
p = p_{ref}\left(\frac{\eta R_d}{p_{ref}}\right)^{cp/cv},
$$

with the prognostic variables: $\tilde\rho' := \sqrt{G'}\rho', \quad \tilde M_x := \sqrt{G'}\rho u, \quad \tilde M_z := \sqrt{G'}\rho w,$

$$
\eta := \rho\Theta, \quad \tilde\eta := \sqrt{G'}\rho\Theta, \quad \tilde\eta' := \tilde\eta - \tilde\eta_0, \quad \tilde\eta_0 := \sqrt{G'}\rho_0\Theta_0,
$$

$$
\tilde p' := \sqrt{G'}p' = \sqrt{G'}(p - p_0),
$$

e.g. Kelly, Giraldo (2012) JCP

A problem with the Euler equations …

Approximate hydrostatic balance

pressure gradient (→flux div.) = buoyancy term (→ source term)

is crucial for the Euler equations.

However, the source term integral contains base polynomials themselves, whereas the flux div. term integral uses *derivatives* of base polynomials.

→ no proper balance possible.

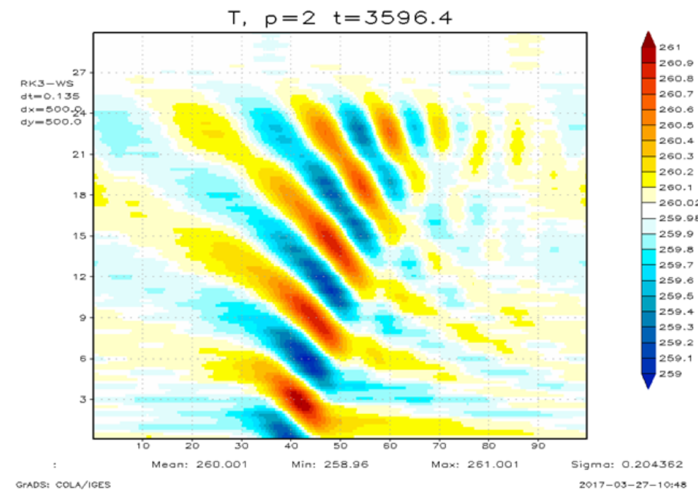

Blaise et al. (2016) IJNMF, Orgis et al. (2017) JCP:

use vertically a reduced base (one polynomial degree less; modal base) for the calculation of the source term.

Test case: cold bubble

Straka et al. (1993)

Test properties:

- test of dry Euler equations (without Coriolis force)
- unstationary
- strongly nonlinear
- comparison with reference solution from paper

DG explicit

no reference state is used!

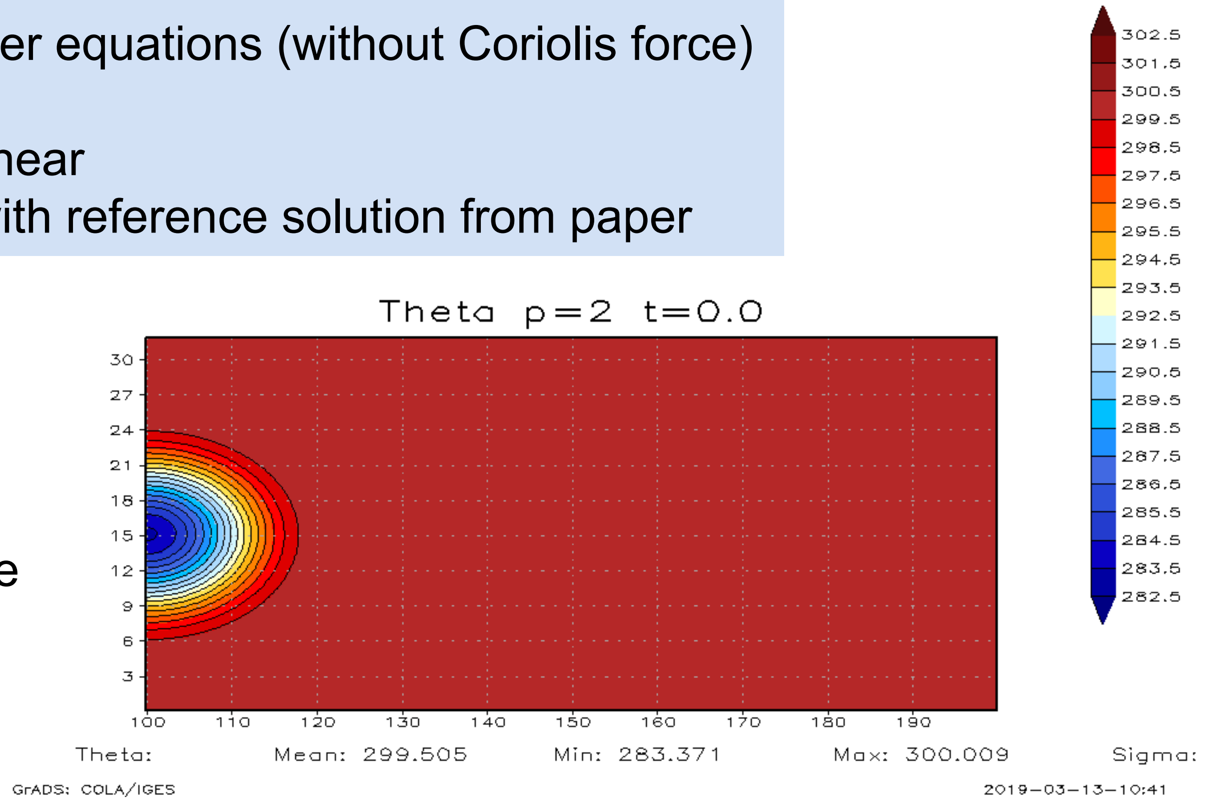

COSMO

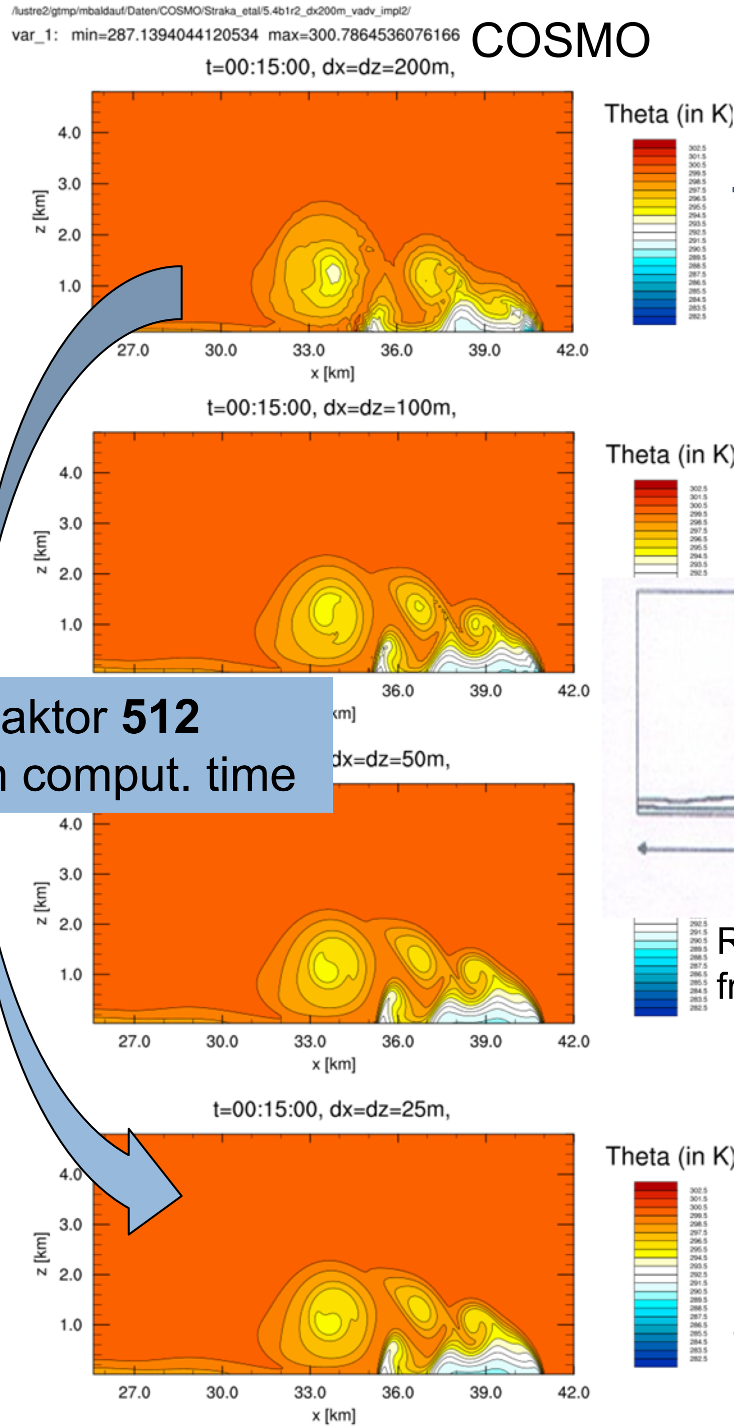

Faktor **512**
in comput. time

DG explicit

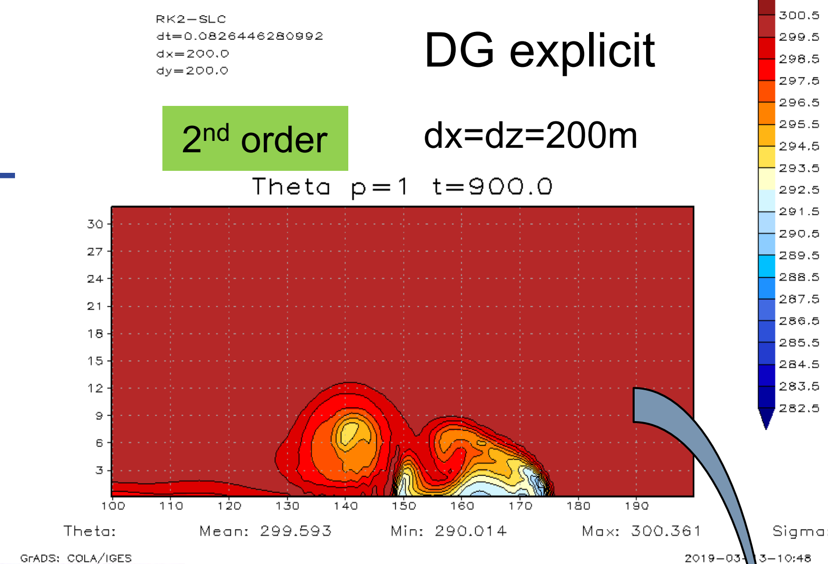

Faktor **4.3**
in comput. time

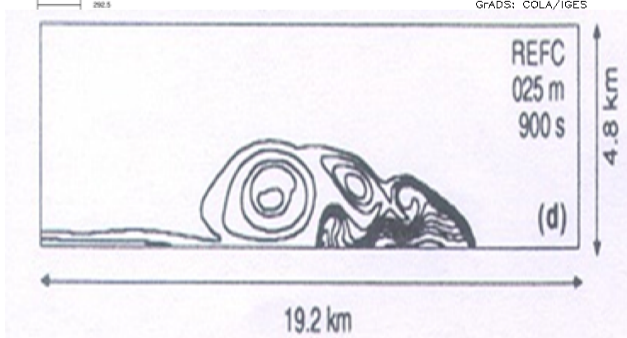

Reference solution
from Straka et al. (1993)

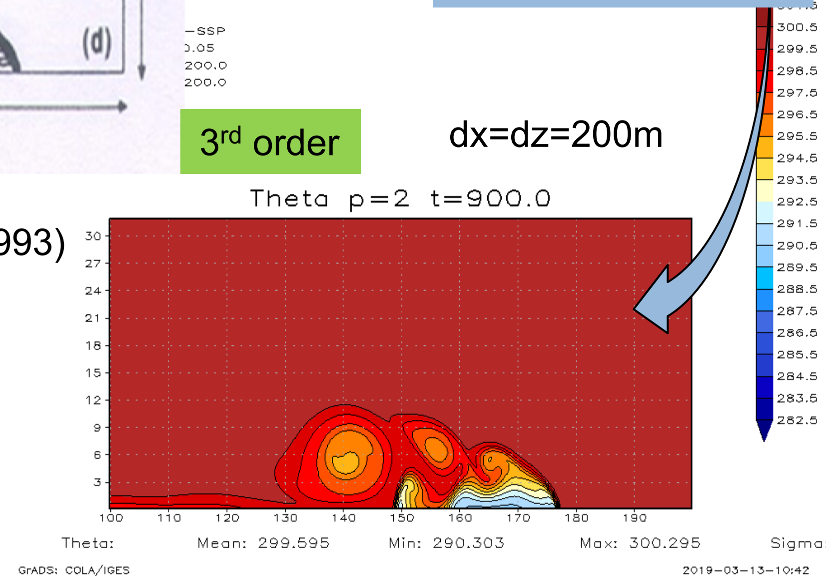

Test case: flow over steep mountains, equidistant grid

Schaer et al. (2002) MWR   (case 5b: U_0=10m/s, N=0.01 1/s)

H_{oro} = 1000m, α_{max} = 38°

H_{oro} = 2000m, α_{max} = 57°

H_{oro} = 3000m, α_{max} = 61°

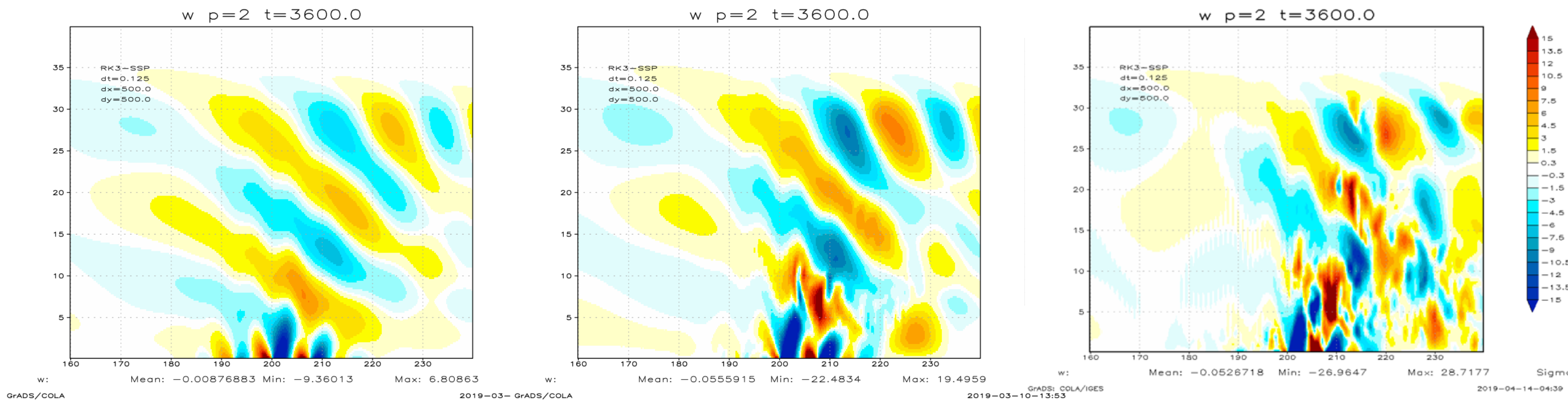

Explicit DG simulation (3rd order) remains stable even for steeper slopes!
(remark: diffusion switched off → strong gravity wave breaking occurs)

Test case: flow over steep mountains, vertically stretched grid

Schaer et al. (2002) MWR (case 5b: U_0=10m/s, N=0.01 1/s)

H_{oro} = 1000m, α_{max} = 38°

H_{oro}= 2000m, α_{max} = 57°

H_{oro} = 3000m, α_{max} = 61°

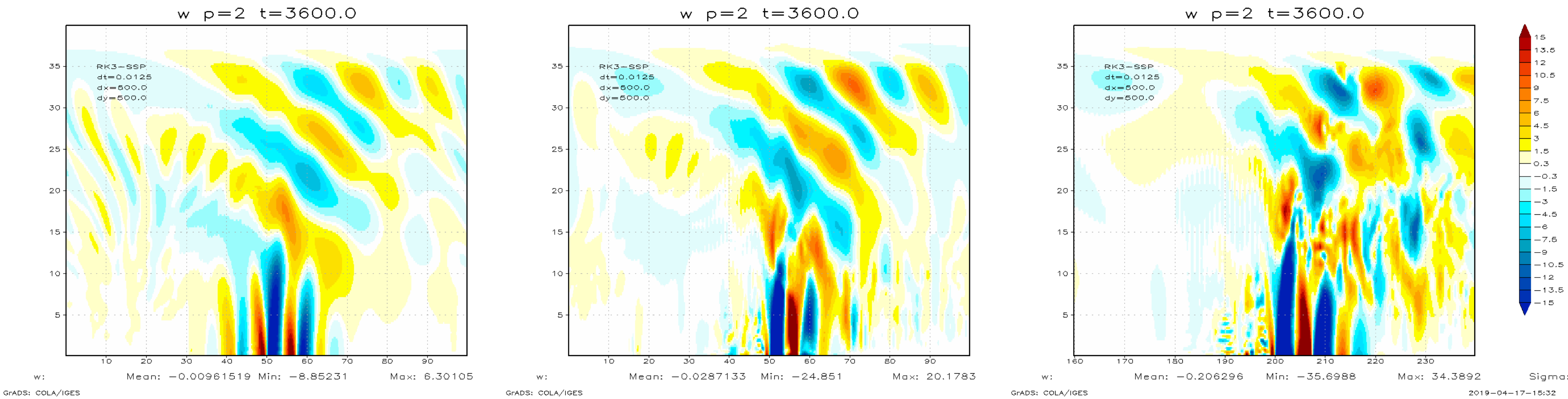

with vertical grid stretching ~1:20, Δz_{min}~50m

Explicit DG simulation (3rd order) remains stable even for steeper slopes!
(remark: diffusion switched off → strong gravity wave breaking occurs)

Linear gravity/sound wave expansion in a channel

Deutscher Wetterdienst
Wetter und Klima aus einer Hand

setup similar to *Skamarock, Klemp (1994) MWR*

Δx=500m, Δz=250m

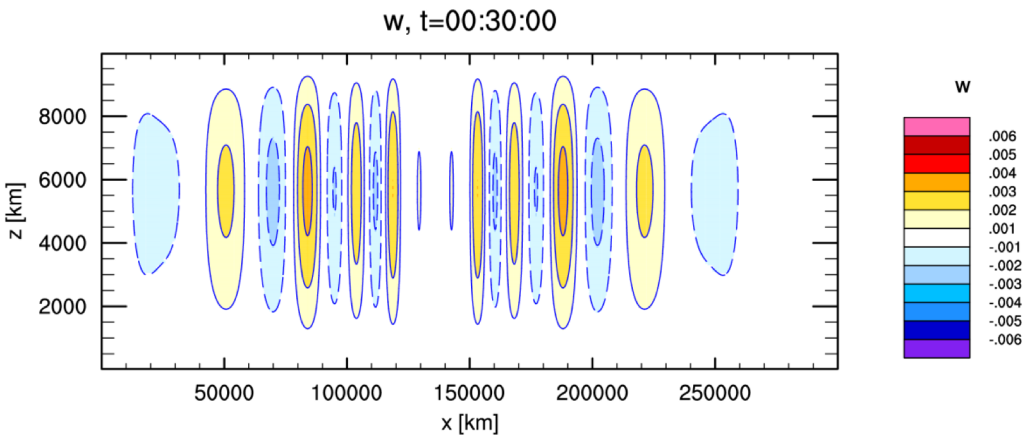

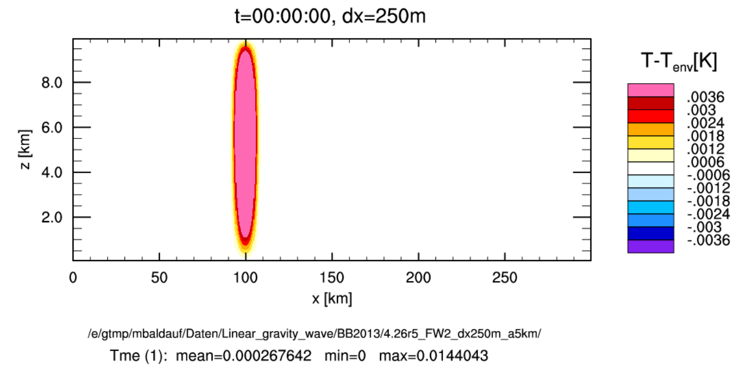

Exact 3rd order convergence for w and T':

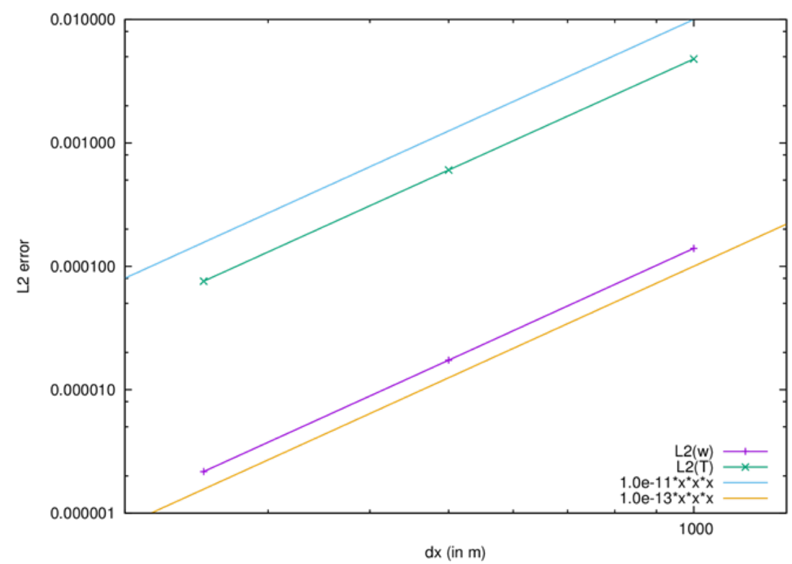

colors : simulation with p=2/RK3-SSP (i.e. 3rd order explicit DG)

blue lines: analytic solution for compressible, non-hydrostatic Euler eqns. (*Baldauf, Brdar (2013) QJRMS*)

Horizontally explicit - vertically implicit (HEVI)-scheme with DG

Motivation: get rid of the strong time step restriction by vertical sound wave expansion in flat grid cells (in particular near the ground)

$$\frac{\partial q^{(s)}}{\partial t} + \underbrace{\nabla \cdot \mathbf{f}^{(s)}_{slow}}_{\text{explicit}} + \underbrace{\nabla \cdot \mathbf{f}^{(s)}_{fast}}_{\text{implicit}} = \underbrace{S^{(s)}_{slow}}_{\text{explicit}} + \underbrace{S^{(s)}_{fast}}_{\text{implicit}}$$

$$\mathbf{f}^{(s)}_{fast} = f^{(s)}_{z,fast} \mathbf{e}_z \qquad\qquad f^{(s)}_{z,fast} = \sum_{s'} H^{ss'} q^{(s')}$$

References:
Giraldo et al. (2010) SIAM JSC: propose a HEVI semi-implicit scheme
Bao, Klöfkorn, Nair (2015) MWR: use of an iterative solver for HEVI-DG
Blaise et al. (2016) IJNMF: use of IMEX-RK schemes in HEVI-DG
Abdi et al. (2017) arXiv: use of multi-step or multi-stage IMEX for HEVI-DG

2D Euler equations, non-hydrostatic, compressible with a reference state, in terrain-following coordinates (x, z‘)

use a *strong conservation form* with terrain following coordinates but cartesian base vectors (*Schuster et al. (2014) MetZ, appendix, for the sphere):*

$$
\begin{aligned}
\frac{\partial \tilde\rho'}{\partial t} + \frac{\partial}{\partial x}(\tilde M_x) + \frac{\partial}{\partial z'}\left(\boxed{\frac{\partial z'}{\partial x}\tilde M_x + \frac{\partial z'}{\partial z}\tilde M_z}\right) &= 0, \\
\frac{\partial \tilde M_x}{\partial t} + \frac{\partial}{\partial x}\left(\frac{\tilde M_x^2}{\tilde\rho} + \tilde p'\right) + \frac{\partial}{\partial z'}\left(\frac{\partial z'}{\partial x}\left(\frac{\tilde M_x^2}{\tilde\rho} + \boxed{\tilde p'}\right) + \frac{\partial z'}{\partial z}\frac{\tilde M_x \tilde M_z}{\tilde\rho}\right) &= 0, \\
\frac{\partial \tilde M_z}{\partial t} + \frac{\partial}{\partial x}\left(\frac{\tilde M_x \tilde M_z}{\tilde\rho}\right) + \frac{\partial}{\partial z'}\left(\frac{\partial z'}{\partial x}\frac{\tilde M_x \tilde M_z}{\tilde\rho} + \frac{\partial z'}{\partial z}\left(\frac{\tilde M_z^2}{\tilde\rho} + \boxed{\tilde p'}\right)\right) &= \boxed{-g\tilde\rho'} - \frac{\tilde M_z}{\tau}, \\
\frac{\partial \tilde\eta'}{\partial t} + \frac{\partial}{\partial x}\left(\frac{\tilde\eta \tilde M_x}{\tilde\rho}\right) + \frac{\partial}{\partial z'}\left(\boxed{\frac{\partial z'}{\partial x}\frac{\tilde\eta \tilde M_x}{\tilde\rho} + \frac{\partial z'}{\partial z}\frac{\tilde\eta \tilde M_z}{\tilde\rho}}\right) &= 0,
\end{aligned}
$$

$$
p = p_{ref}\left(\frac{\eta R_d}{p_{ref}}\right)^{cp/cv},
$$

$\boxed{}$ **= terms treated implicitly** (after linearizsation)

Some remarks about the DG-HEVI approach

- Treatment of the local Lax-Friedrich flux:

$$\left(\mathbf{f}^{(s)}_{slow} + \mathbf{f}^{(s)}_{fast}\right)^{(num)} \cdot \mathbf{n} = \frac{1}{2}\left(\mathbf{f}^{(s)}_{slow,+} + \mathbf{f}^{(s)}_{slow,-} \overbrace{+ \mathbf{f}^{(s)}_{fast,+} + \mathbf{f}^{(s)}_{fast,-}}^{\text{implicit}}\right) \cdot \mathbf{n}$$

$$- \frac{\lambda_{slow}}{2}\left(q^{(s)}_{+} - q^{(s)}_{-}\right) \underbrace{- \frac{\lambda_{fast}}{2}\left(q^{(s)}_{+} - q^{(s)}_{-}\right)}_{\text{implicit}}$$

Blaise et al. (2016) IJNMF

- Use of IMEX-RK (SDIRK) schemes: SSP3(3,3,2), SSP3(4,3,3) (*Pareschi, Russo (2005) JSC*)
- The implicit part leads to several band diagonal matrices → here a direct solver is used (expensive!)
- Until now a modal base is used (not necessary, but tensor product seems advisable)
- BCs: reflective and mirror conditions are applied in a weak form (experience: for explicit terms only mirror conditions)

Test case: falling cold bubble (Straka et al. (1993)
Comparison explicit vs. HEVI scheme

DG explicit | DG HEVI

2nd order

3rd order

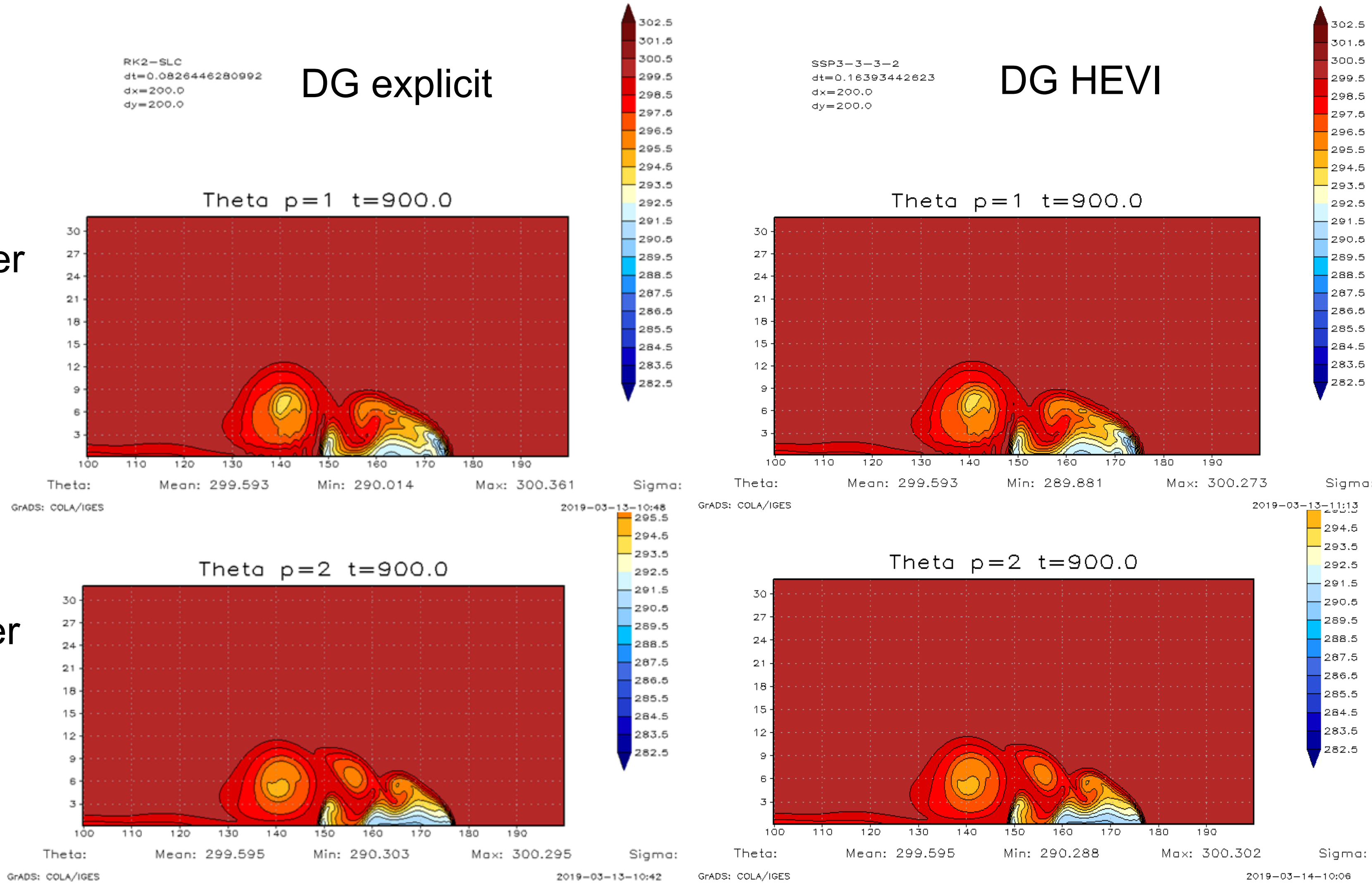

test case: linear gravity/sound wave expansion in a channel

DG explicit
3rd order
dx=500m, dz=250m

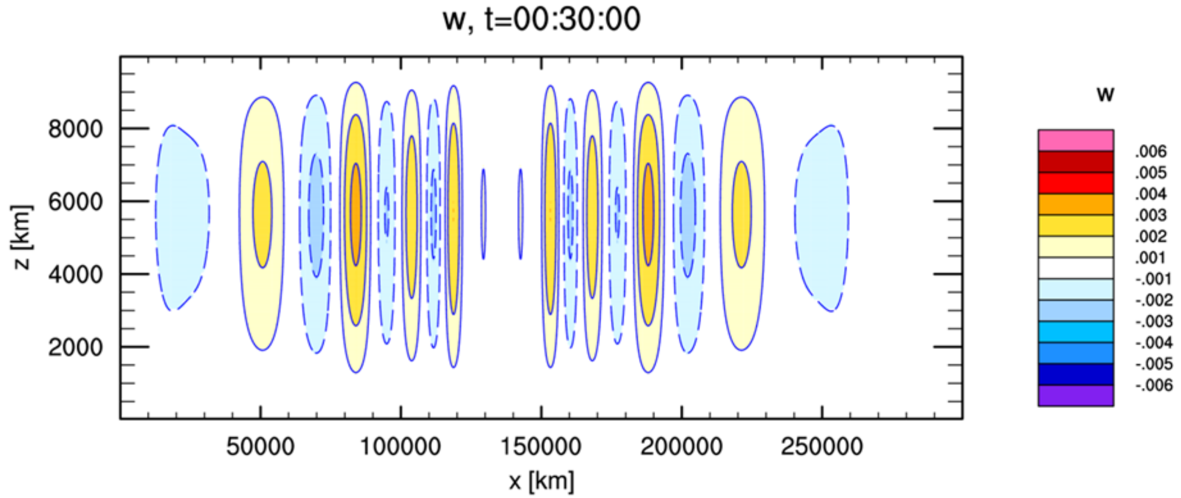

DG HEVI
3rd order
dx=1000m, dz=500m

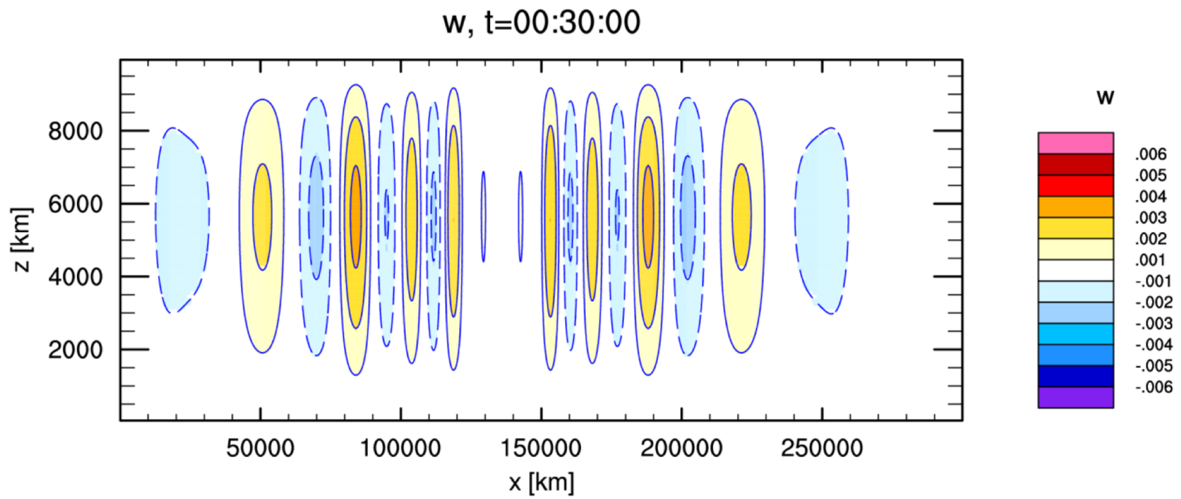

First attempts to bring it on the sphere …

Idea to avoid pole problem and to keep high order discretization:
use **local (rotated) coordinates** for every (triangle) grid cell,
i.e. rotate every grid cell towards $\lambda \approx 0$, $\varphi \approx 0$.
→ geometry is treated exactly
→ transform fluxes between neighbouring cells

Example: 2D scalar advection equation on the sphere

$$\frac{\partial}{\partial t}\sqrt{G}\rho + \frac{\partial}{\partial x^i}\sqrt{G}v^i\rho = 0$$

x^i = rotated geographical – gnomonial coordinates

Läuter, Giraldo et al. (2007): shift $\sqrt{G}$ into the integral (e.g. to calc. the mass matrix) and treat ρ as the prognostic variable

Test case: scalar advection on a sphere with a prescribed velocity field for **solid body rotation** with ω=0.1/s, rotation axis tilted by 45°

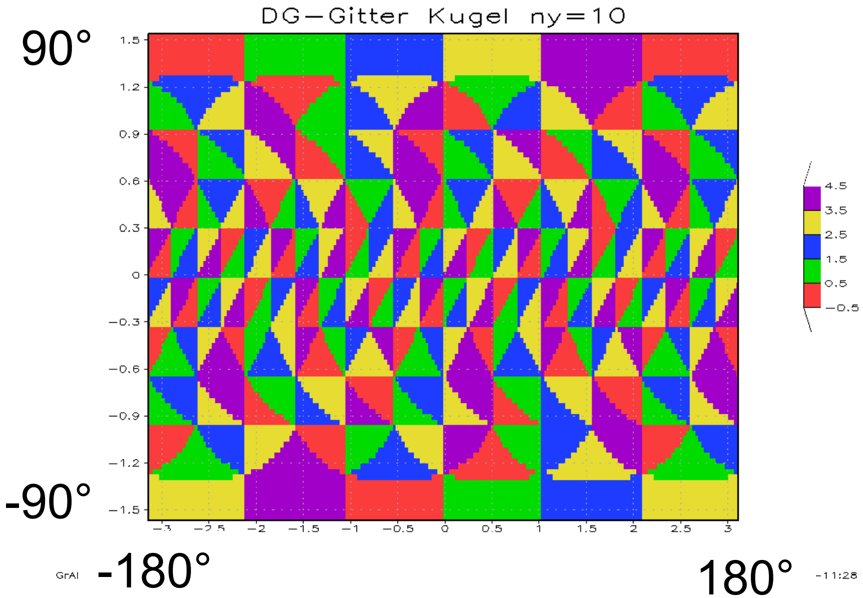

simple triangle grid on the sphere

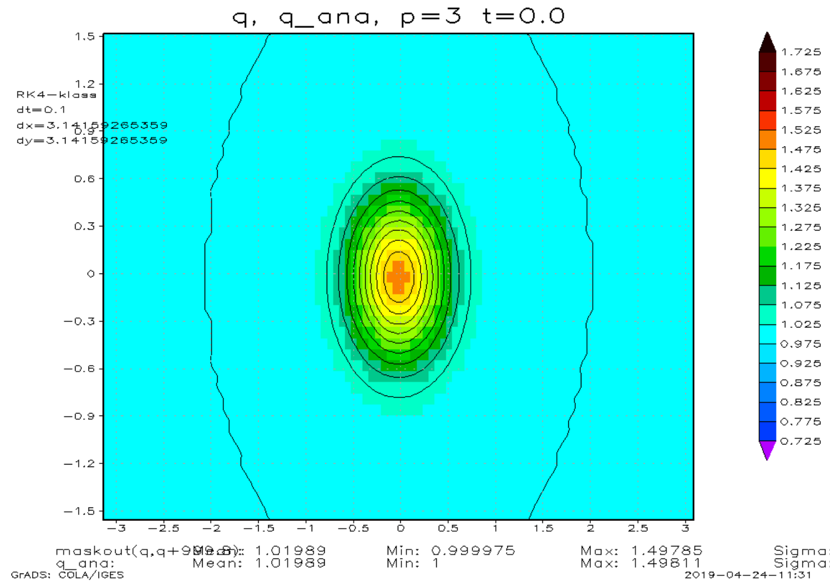

4th order scheme (with RK4) transport is mass conserving (up to roundoff precision)

Analogous: shallow water equations on the sphere

covariant formulation (here: without bathymetry)

$$
\begin{aligned}
\frac{\partial \sqrt{G} H}{\partial t} + \frac{\partial}{\partial x^i} \sqrt{G} m^i &= 0 \\
\frac{\partial \sqrt{G} m^i}{\partial t} + \frac{\partial}{\partial x^j} \sqrt{G} T^{ij} &= \sqrt{G} (F^i_{Cor} - \Gamma^i_{jk} T^{jk}) \\
T^{ij} &= \frac{m^i m^j}{H} + \frac{1}{2} g^{ij} g_{grav} H^2
\end{aligned}
$$

Shallow water equations on the sphere:

Rossby-Haurwitz wave (test case 6 in *Williamson et al. (1992)*)

initialisation:

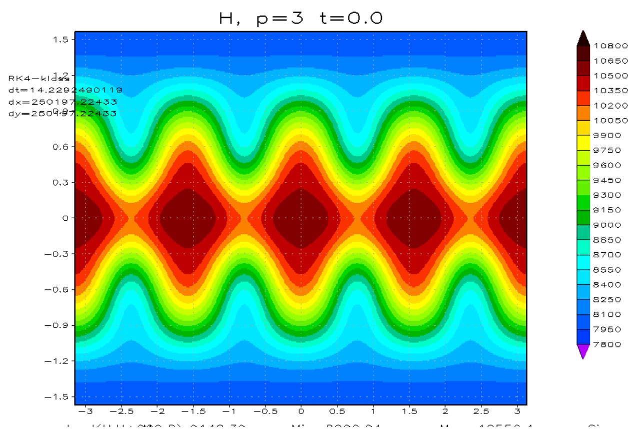

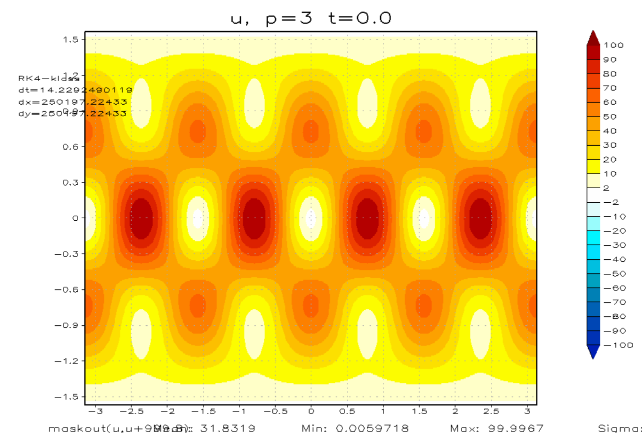

after 24h:

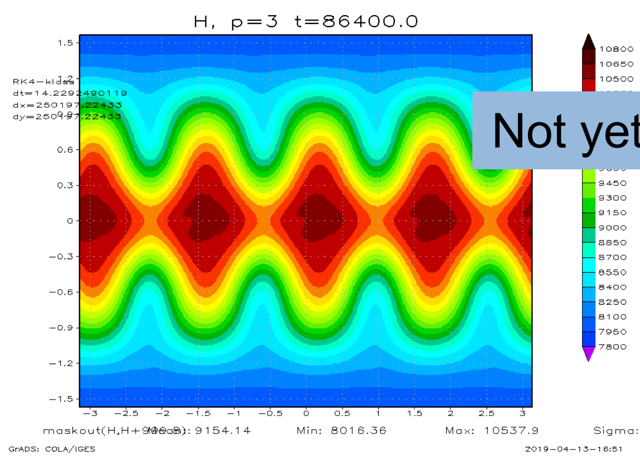

Not yet satisfying …

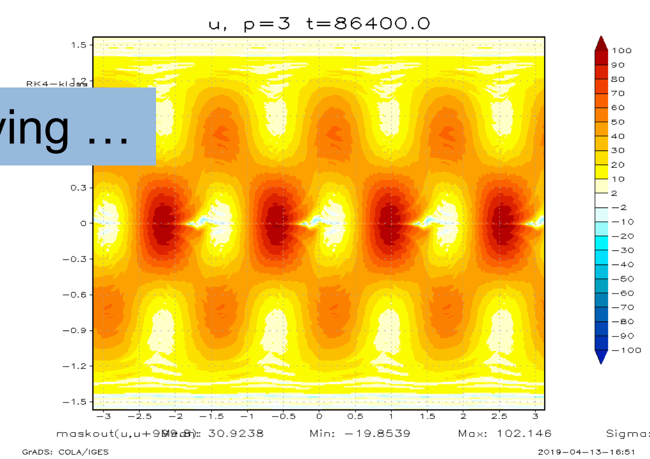

Summary

- 2D toy model for
  - explicit DG-RK (on arbitrary unstructured grids with triangle or quadrilateral grid cells) and
  - HEVI DG-IMEX-RK

  works for several idealized tests (also Euler equations with terrain-following coordinates) correct convergence behaviour, …
- problems with well-balancing solved
- no reference state necessary (← higher accuracy)
- HEVI-DG: treatment of numerical flux and boundary conditions seems to work, too.
  Band diagonal (direct) vertical solver is expensive (for 2D simul./p=2, needs ~40% of total comput. time)
- DG on the sphere by use of local (rotated gnomonial) coordinates

Outlook

- work in progress → several bug fixes in the 2D toy model necessary (e.g. lower BCs for DG-HEVI with mountains, local transformations on the sphere, …)
- take further design decisions:
  nodal vs. modal DG, local DG vs. interior penalty vs. …, …
- coupling of tracer advection (mass-consistency)?
- improve efficiency in the HEVI direct solver:
  use of block-tridiagonal structure of the band diagonal matrices?
- further milestones at DWD (for the next years!)
  - development of a 3D prototype DG-HEVI solver
  - choose optimal convergence order p
    estimated: $p_{horiz} \sim 3 \dots 6$, $p_{vert} \sim 3 \dots 4$ ($p_{time} \sim 3 \dots 4$)

How to treat orography and how to bring DG on the sphere?

For local models: use a *strong conservation form* with
spherical + terrain following coordinates but spherical base vectors
Schuster et al. (2014) MetZ (appendix):

for a scalar field Ψ:

$$\frac{\partial \sqrt{G'}\Psi}{\partial t} + \frac{\partial}{\partial x^{k'}} \left(\sqrt{G'} f^{*k} \frac{\partial x^{k'}}{\partial x^k} \frac{1}{\sqrt{g_{(kk)}}} \right) = \sqrt{G'} S.$$

vor a vector field m:

$$\frac{\partial \sqrt{G'} m^{*k}}{\partial t} + \frac{\partial}{\partial x^{j'}} \left(\sqrt{G'} \frac{\partial x^{j'}}{\partial x^i} \frac{1}{\sqrt{g_{(ii)}}} T^{*k*i} \right) = \sqrt{G'} (S^{*k} - b^{*k})$$

*=physical (contravariant) components
b*='non-flux-form'-corrections of momentum flux due to spherical metric terms

~~For the whole sphere: use the icosahedral/triangle grid of ICON together with vector, tensor components mentioned above~~